ELSEVIER

Contents lists available at SciVerse ScienceDirect

Applied Catalysis A: General

journal homepage: www.elsevier.com/locate/apcata



Gas phase hydrogenation of maleic anhydride at low pressure over silica-supported cobalt and nickel catalysts

Camilo I. Meyer¹, Silvina A. Regenhardt, Alberto J. Marchi, Teresita F. Garetto*

Catalysis Science and Engineering Research Group (GICIC), Instituto de Investigaciones en Catálisis y Petroquímica (INCAPE), FIQ-UNL-CONICET, Santiago del Estero 2654 (3000) Santa Fe. Argentina

ARTICLE INFO

Article history:
Received 4 October 2011
Received in revised form
13 December 2011
Accepted 15 December 2011
Available online 24 December 2011

Keywords: Selective hydrogenation Maleic anhydride γ-Butyrolactone Metal-based catalysts

ABSTRACT

The gas-phase hydrogenation of maleic anhydride over Ni/SiO₂ and Co/SiO₂ catalysts, prepared by the incipient wetness impregnation method, was studied. The catalytic tests were carried out at 1 bar pressure, between 170 and 220 °C and W/F_{MA}^0 in the range 5–25 g h mol⁻¹. In this work, the product distribution was different to those obtained at high pressures, previously reported in the open literature. $Both \ Ni/SiO_2 \ and \ Co/SiO_2 \ catalysts \ were \ active \ for \ the \ selective \ hydrogenation \ of \ maleic \ anhydride \ (MA)$ into succinic anhydride (SA). Subsequently, SA was converted to γ -butyrolactone (GBL) and propionic acid (PA). Neither tetrahydrofurane nor butanediol were detected at the reactor outlet. GBL/PA ratio was strongly depending on the metallic catalyst and temperature. At 170 °C, Ni/SiO₂ was more selective to GBL than Co/SiO₂. Besides, with Ni/SiO₂, GBL formation rate diminished during the experiment while PA production showed a small increase. Instead, over Co/SiO₂, both the PA and GBL formation rate decayed with time on stream. At 220 °C, Co/SiO₂ showed a higher initial selectivity to GBL than Ni/SiO₂. However, the GBL formation rate diminished more rapidly with Co/SiO₂ than with Ni/SiO₂. Thus, both catalysts gave similar selectivity to GBL after 3 h reaction at 220 °C. The observed catalyst deactivation was attributed to carbonaceous species of different nature deposited on the metallic phase during reaction. The amount and type of these species depends on both metal catalysts and reaction conditions. Selectivity and stability of Ni/SiO₂ and Co/SiO₂ catalysts is explained on the basis of their hydrogenolytic activity.

© 2011 Elsevier B.V. All rights reserved.

1. Introduction

The main products in the gas phase hydrogenation of maleic anhydride (MA) are succinic anhydride (SA), γ -butyrolactone (GBL), tetrahydrofurane (THF) and butanediol (BDO) The reaction network for the gas-phase MA hydrogenation is rather complex and different type of reactions can occur, depending on the catalyst and reaction conditions [1,2]. In a first step, the hydrogenation of the C=C bond in MA produces SA. Then, the hydrogenolysis of one C=O bond in SA gives GBL. Finally, THF and BDO can be obtained by GBL hydrogenolysis. Other hydrogenolysis reactions can also produce C_4 and C_3 compounds, such as n-butanol, n-propanol, butyric acid and propionic acid (PA). Most of the compounds mentioned above are mainly employed as solvents, especially to replace the non ecofriendly chlorinated solvents. GBL, PA, THF and BDO are important intermediates in the chemical industry, as well. For example, GBL is used in the synthesis of pyrrolidone and N-methylpyrrolidone,

which are employed for production of agrochemicals, pharmaceuticals and polymers. THF, BDO and PA are used as intermediates for the production of polymers, pesticides and pharmaceuticals. PA is also employed as mold and bacteria inhibitor for animal feed and human food [3,4].

The use of different catalysts, based on both noble and non-noble metals, was reported in the literature for the hydrogenation of MA [1–5,8–24]. Copper-based catalysts modified by Zn, Cr, Ce and Zr were employed for the MA hydrogenation in gas phase [6,7,12,13]. However, Cu loadings as high as 40–60%, high catalyst/reactive ratios and/or high pressures were necessary to obtain high GBL yields. In addition, Cr-based catalysts are not desirable due to the high toxicity of this metal. The liquid-phase hydrogenation of MA was widely studied and high pressures and high temperatures are required to obtain yields in GBL near 40–50% [2,10,14–19].

In a previous paper, we reported the gas-phase hydrogenation of MA over $Cu(10\%)/SiO_2$, prepared by the incipient-wetness impregnation method, at 1 bar and 170–220 °C. After activation under H_2 flow, a phase formed by large metal copper particles was obtained. This catalyst was active and selective in the hydrogenation of MA into SA. However, only very small amounts of GBL were obtained through hydrogenolysis of SA. Besides, this catalyst suffered a rapid

^{*} Corresponding author. Tel.: +54 342 4533858; fax: +54 342 4531068. E-mail address: tgaretto@fig.unl.edu.ar (T.F. Garetto).

¹ Present address: Instituto de Desarrollo Tecnológico para la Industria Química (INTEC) UNL-CONICET.

deactivation due to carbonaceous residues deposited on the metal surface [20].

To the best of our knowledge, there are few papers dealing with the MA hydrogenation in gas phase over Ni and/or Co-based catalysts. In previous works, the hydrogenation of MA on Ni/HY-Al₂O₃ and Ni-Pt/HY-Al₂O₃ gave as main products SA and GBL [21,22]. No other products, such as PA, CH₄ and/or THF, were detected. Selectivities to SA between 60 and 90% at 100% MA conversion were reported. Besides, the catalyst deactivation was attributed to water adsorption. However, a systematic study to determine the real causes for catalyst deactivation was not carried out in that work [21]. On the other hand, it is worth noting that the operation conditions, preparation method of the catalyst and support are very different to the ones used in our work. Generally, MA hydrogenation over nickel or cobalt-based catalysts was carried out mainly in liquid-phase at pressures higher than 10 bar. In this work, we analyze the behavior of Ni/SiO₂ and Co/SiO₂ catalysts in the gas-phase hydrogenation of MA at atmospheric pressure and temperatures in the range of 170-220 °C. The main objective is to establish the feasibility of converting MA into GBL over Ni/SiO2 and Co/SiO2 catalysts with low metal-loading, at high MA conversions and operating under mild conditions.

2. Materials and methods

Ni/SiO $_2$ and Co/SiO $_2$ catalysts were prepared by the incipient-wetness impregnation method. A 0.5 M aqueous solution of the corresponding metal nitrate was added drop by drop at room temperature to the solid support (SiO $_2$, Grace-Davison, 99.7% purity), while stirring. The impregnated samples were dried first at room temperature and then at 110 °C for 12 h. Then, the hydrated precursor thus obtained was thermally treated in air at 500 °C for 6 h.

Elemental compositions were measured by inductively coupled plasma (ICP), using a PerkinElmer Optima 2100 DV spectrometer. The specific surface area (S_g), pore volume (V_p) and mean pore diameter (d_p) of the calcined samples were measured by N_2 physisorption at $-196\,^{\circ}$ C, with a Quantachrome Accusorb S-1 sorptometer. S_g was estimated by employing the BET equation and the pore distribution were determined by applying the BJH method. Previously to N_2 physisorption, samples were degassed under vacuum at $250\,^{\circ}$ C.

The metallic nickel dispersion was determined by hydrogen chemisorption. The volumetric adsorption experiments were performed at $25\,^{\circ}\text{C}$ in a conventional vacuum unit equipped with an MKS Baratron pressure gauge. Catalysts were reduced at $500\,^{\circ}\text{C}$ for $2\,\text{h}$ and then outgassed $2\,\text{h}$ at $500\,^{\circ}\text{C}$ prior to performing H_2 chemisorption experiments [23].

The crystalline species formed in the calcined samples were identified by using X-ray diffraction (XRD), in the 2θ range of $10-70^\circ$ at a scan speed of 2° min⁻¹, using a Shimadzu D1 diffractometer and Ni-filtered Cu K α radiation (λ = 0.1540 nm). TPR profiles were obtained in a Micromeritics AutoChem 2920 system, equipped with a TCD detector and using $H_2(5\%)/Ar$ with a volumetric flow rate of 60 mL min⁻¹ STP. The sample (100 mg) was heated from 25 °C to 700 °C at 10 °C min⁻¹.

Catalytic activity tests were carried out at atmospheric pressure in a stainless steel fixed-bed tubular reactor. Samples were pressed to obtain tablets which then were crushed and screened. The reactor was loaded with 20–150 mg of catalyst (W), having a particle size in the 0.35–0.42 mm range, diluted in quartz. Diffusional limitations were ruled out by varying the particle size in the range of 0.15–0.60 mm and the space time between 5 and 40 g catalyst h mol⁻¹. Prior to the activity tests, catalysts were activated in situ by reduction in H₂ flow at 500 °C for 1 h. Then, the reactor was cooled down to the reaction temperature. Once the reaction

Table 1Physicochemical properties of the silica-supported metal samples.

Sample	$S_{\rm g} \ ({\rm m}^2 \ {\rm g}^{-1})$	$V_{\mathrm{p}}~(\mathrm{cm^3~g^{-1}})$	Metal load (wt.%)	Dispersion (%)
SiO ₂	254	0.880	_	_
Ni/SiO ₂	250	0.851	9.65	2.50
Co/SiO ₂	252	0.865	9.21	n.d

temperature was stabilized, a $\rm H_2$ stream saturated in MA at 70 °C, in order to obtain a $\rm H_2/MA$ molar ratio of about 130, was fed to the stainless steel reactor. Catalytic tests were carried out between 170 and 220 °C, at atmospheric pressure, using space times ($W/F_{\rm MA}^0$) in the range 5–25 g catalyst h mol⁻¹. On-line analysis of the reactor outlet stream was performed using a Varian CP 3380 gas chromatograph equipped with a flame ionization detector and a Graphpac GC 0.1% AT-1000 (80–100) packed column.

After the catalytic test, the used catalysts were analyzed by temperature-programmed oxidation (TPO). The experiments were performed in the temperature range of 25–800 °C, with a heating rate of $10\,^{\circ}\text{C}\,\text{min}^{-1}$, and using an $O_2(1\%)/N_2$ stream at $60\,\text{mL}\,\text{min}^{-1}$ as the oxidant mixture. The CO_2 exiting the TPO reactor was converted to methane in a reactor loaded with a Ni/Kieselghur catalysts, operating a $400\,^{\circ}\text{C}\,\text{in}\,\text{H}_2$ flow [28]. The methanator outlet was monitored using a flame ionization detector (FID). Data acquisition was carried out by using Peak 356 software. Calibration was made using a reference catalyst having a known amount of coke [20].

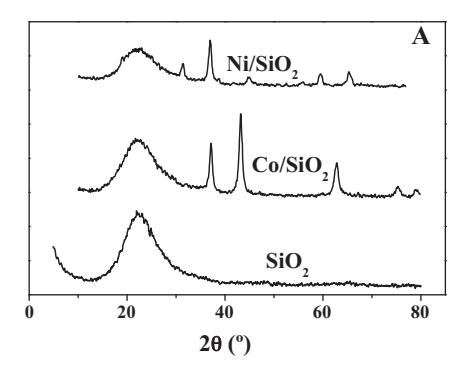
3. Results and discussion

3.1. Physicochemical characterization

The main physicochemical characteristics of Ni/SiO $_2$ and Co/SiO $_2$ samples are shown in Table 1 and Fig. 1. After impregnation and calcination, the metal load was between 9 and 10% in both samples and the specific surface area S_g and V_p of the support did not suffer substantial modifications. In the case of the Ni/SiO $_2$ sample, after reduction in H $_2$ at 500 °C, a metallic nickel dispersion of 2.5% was determined by H $_2$ chemisorption. A mean size of 40.5 nm was estimated by assuming a cubic symmetry for the metallic nickel particles.

Fig. 1A shows the corresponding X-ray diffractograms for the silica, used as support, and for the Co/SiO_2 and Ni/SiO_2 calcined samples. Only the characteristic amorphous halo, between 15 and 30° , was observed for the silica sample. A polycrystalline phase assigned to Co_3O_4 with a spinel-like structure (Co_3O_4 , JCPDS 9-418) could be detected in the case the Co/SiO_2 sample. Similarly, for Ni/SiO_2 sample, a NiO polycrystalline phase (NiO, JCPDS 22-1189) was observed after calcination. The crystallite sizes, estimated using Debye–Scherrer equation, were 11 nm for Co_3O_4 and 10 nm for NiO. The large crystallite sizes, estimated from the corresponding XRD patterns of both samples, are in agreement with the large particle size determined by H_2 chemisorption in the case of Ni/SiO_2 sample.

The TPR profiles for the calcined Ni/SiO₂ and Co/SiO₂ samples are presented in Fig. 1B. A single broad reduction peak, with a maximum at 395 °C, was observed with Ni/SiO₂. This peak may be assigned to the reduction of large particles of NiO [24]. In the case of the Co/SiO₂ sample, two reduction peaks were observed. The first peak, with a maximum at 295 °C, could be assigned to the reduction of Co₃O₄ to CoO. The second peak, having a maximum around 360 °C, corresponds to the reduction of CoO to Co⁰ [25]. It was determined that a 95% of the nickel oxide phase, obtained by incipient wetness impregnation and posterior calcination, was reduced to metal nickel. This value was estimated by the ratio between the experimental H₂ consumption calculated from TPR profiles performed up to 500 °C and the theoretical H₂ consumption calculated



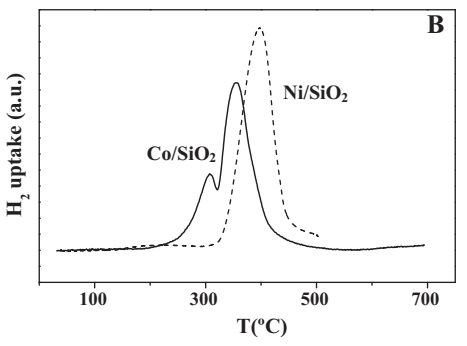


Fig. 1. XRD patterns (A) and TPR profiles (B) of the samples calcined in an air stream at 500 °C.

from NiO content. A similar level of reduction was verified in the case of Co/SiO_2 oxide precursors estimated using the same method [26]. These results are indicating a slightly interaction between oxide phase and silica support and they are in agreement with those observed in previous works for similar samples obtained by the incipient wetness method, having 8% metal loads [27]. The results obtained by TPR are in a good agreement with those obtained by XRD and dispersion measurements.

In summary, according to the characterization results, both the Ni/SiO₂ and Co/SiO₂ samples used in this work are constituted by large metal particles having low interaction with the support. Both metallic phases were formed by reduction, under H₂ flow at T < 500 °C, of polycrystalline NiO and Co₃O₄ on silica surface.

3.2. Catalytic tests

Initially, several experiments over Ni/SiO₂ at 170 and 195 °C, varying the space time $(W/F_{\rm MA}^0)$ between 5 and 25 g catalyst $h \, mol^{-1}$, were performed. The results are summarized in Table 2. It is worth noting that MA can be very easily hydrogenated into SA and the initial MA conversion was significantly lower than 100% only at 170 °C and when the space time was lower than 10 g catalyst h mol^{-1} . In these conditions, the only product detected was SA. As the space time and the MA conversion increased, GBL, PA and CH₄ were also observed at the reactor outlet stream. Moreover, the yield in SA reached a maximum and then diminished as the space time was increased, while the yield in GBL and PA increased continuously, in the same amount that the yield in SA diminished. These results are indicating that the reaction sequence (Fig. 2) is as follows: (1) first, MA is hydrogenated into SA; (2) SA is subsequently converted to GBL and PA by different hydrogenolysis reactions. It is also likely that some GBL might be converted into PA.

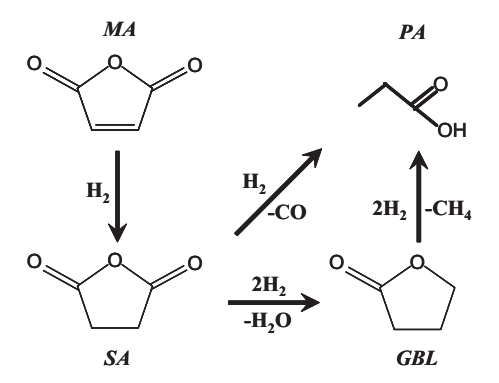


Fig. 2. Reaction network for the maleic anhydride hydrogenation. MA: maleic anhydride; SA: succinic anhydride; GBL: γ-butyrolactone; PA: propionic acid.

The catalytic performance of Ni/SiO₂ and Co/SiO₂ was compared at 170 and 220 °C, using a space time of 11.9 g catalyst h mol $^{-1}$. At 170 °C, using Ni/SiO₂ as catalyst, the MA conversion was constant between 95 and 100% along the 3 h reaction test. Instead, with Co/SiO₂, MA conversion dropped fast from about 75 to 40% reaching the steady state in just 1.5 h. These results are indicating that, for similar experimental conditions, Co/SiO₂ is less active and stable than Ni/SiO₂ catalyst in the gas-phase hydrogenation of MA into SA. At 220 °C, the initial MA conversion was 100% with Ni/SiO₂ and Co/SiO₂, remaining constant along the 3 h reaction test.

Considering that hydrogenation of MA to SA and hydrogenolysis of SA to GBL and PA are consecutive reactions (Fig. 2), the SA conversion into GBL and PA was estimated. In all of the cases, SA conversion values lower than 100% were obtained for the experimental conditions used in this work. The evolutions for SA conversion at 170 °C are shown in Fig. 3A. With Ni/SiO₂, SA conversion kept constant around 13% during the 3 h reaction test. Instead, with Co/SiO₂, the SA conversion decayed from almost 30% to about 20% in less than one hour, reaching then a steady state. Thus, at 170 °C, Co/SiO₂ showed a higher initial activity for SA hydrogenolysis but lower stability than Ni/SiO₂. The SA conversion as a function of time at 220 °C is shown in Fig. 3B. When Ni/SiO₂ was used as catalyst, SA conversion increased slightly from 68 to 71% in about

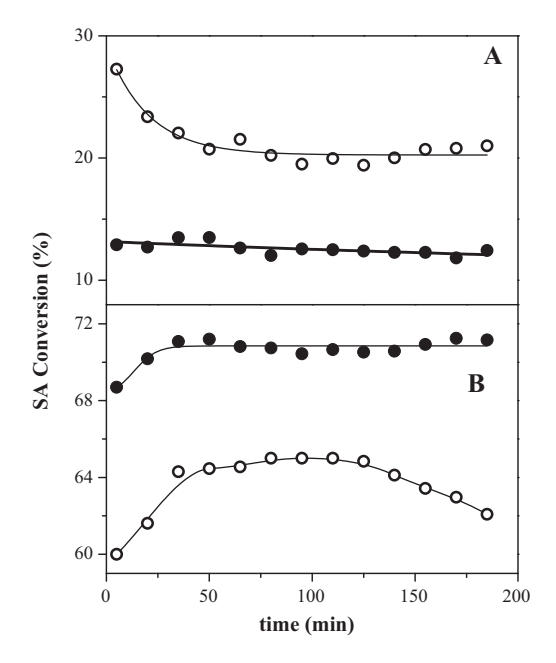


Fig. 3. Succinic anhydride conversion as a function of time at $170\,^{\circ}$ C (A) and $220\,^{\circ}$ C (B). P=1 bar, $W/F_{\rm MA}^0=11.9$ g catalyst h ${\rm mol}^{-1}$, ${\rm H}_2/{\rm MA}=130$, (\bullet) Ni/SiO₂, (\bigcirc) Co/SiO₂.

Table 2 Gas-phase hydrogenation of maleic anhydride (MA) over Ni/SiO_2 at different temperatures and space times (P = 1 bar).

T (°C)	W ^a (mg)	$W/F_{\rm MA}^0$ (g h mol ⁻¹)	<i>X</i> _{MA} ^b (%)	Y _{SA} ^c (%)	Y _{GBL} ^c (%)	Y _{PA} ^c (%)	Y _{CH4} ^c (%)
170	25	5.8	67.9	67.9	n.d.	n.d.	n.d.
	50	11.9	96.5	87.1	5.8	3.6	n.d.
	100	23.8	97.7	79.9	10.7	6.5	0.6
195	50	11.9	100.0	65.5	17.5	15.6	1.4
	100	23.8	100.0	53.8	24.5	20.0	1.7

- a Mass of catalyst.
- ^b Maleic anhydride conversion.
- ^c Product yield.

45 min and then it remained constant. In the case of Co/SiO₂, the evolution was some more complex: first, SA conversion increased from about 60 to 65% in 50 min, then it remained constant for almost 1 h and finally it diminished slowly. Thus, when the reaction was carried out at 220 °C, Ni/SiO₂ showed higher hydrogenolytic activity than Co/SiO₂, which is the opposite to that observed at 170 °C. In addition, Ni/SiO₂ showed a more stable behavior than Co/SiO₂ during the whole experiment. Then, Co/SiO₂ seems to be a less stable catalyst than Ni/SiO₂ for the gas phase hydrogenation of MA.

In all cases, the only hydrogenolysis products detected were GBL, PA and CH₄. THF and BDO were never observed in the experimental conditions used in this work. At 170 °C, the main hydrogenolysis products were PA and GBL (Fig. 4). The evolutions for SA hydrogenolysis rate are shown in Fig. 4A. Initial SA conversion rate was almost three times higher with Co/SiO₂ than with Ni/SiO₂. However, while SA conversion rate diminished with time on stream when Co/SiO₂ was used as catalyst, it kept rather constant with Ni/SiO₂. Initial GBL production rate was similar for Ni/SiO₂ and Co/SiO₂ and then it diminished until a steady state was reached (Fig. 4B). The diminution of GBL production rate was some more important with Co/SiO₂ than with Ni/SiO₂. Thus, the GBL production rate at the steady state was some higher for Ni/SiO₂ than for Co/SiO₂. The evolution of PA production rate with time on stream was rather different for both catalysts (Fig. 4C). In the case of Co/SiO2, the PA formation rate diminished with time on stream until a steady state was reached, similar to the evolution observed for SA and GBL (Fig. 4A and B). Instead, with Ni/SiO₂, the PA production rate increased during the first 50 min and then it kept almost constant. This evolution is also qualitatively similar to that of SA conversion rate (Fig. 4A) but different to the one observed for GBL production rate (Fig. 4B). Very small amounts of CH₄ were also detected at 170 °C and atmospheric pressure. For each catalyst, the CH₄ production rate was about one order lower than GBL and PA production rates (Fig. 4D). The evolution with time was similar to that observed for PA (Fig. 4C) and completely different to that for GBL (Fig. 4B). In principle, there are two possible ways to produce this methane: (1) from GBL hydrogenolysis; (2) by partial hydrogenation of CO produced from SA hydrogenolysis (Fig. 2). In any case, it is clear that the GBL conversion into PA and CH₄ is very low. However, considering the evolutions shown in Fig. 4, it is more likely that the main methane source is the partial hydrogenation of CO over the metal surface. Then, the main PA source must be the SA hydrogenolysis.

The results described above are in agreement with the fact that SA hydrogenolysis to GBL and PA are following parallel pathways (Fig. 2). Moreover, when Ni/SiO₂ was used as catalyst, it is very clear that SA hydrogenolysis to GBL is affected in a different way than the decarbonylation into PA, since while GBL production rate decreases with time on stream (Fig. 4B), PA and CH₄ production rates increases slightly and then it kept constant with time (Fig. 4C and D). The initial $r_{\rm GBL}/r_{\rm PA}$ ratio is 2 (Fig. 5A), i.e. almost 67% of the SA is initially converted into GBL. Then, the $r_{\rm GBL}/r_{\rm PA}$ ratio diminished until both production rates became similar. The different evolutions for GBL and PA production rates over Ni/SiO₂ catalyst is suggesting that both reactions are taking place on different types of hydrogenolytic metal sites. Thus, while the active sites for SA hydrogenolysis into GBL were deactivated during the

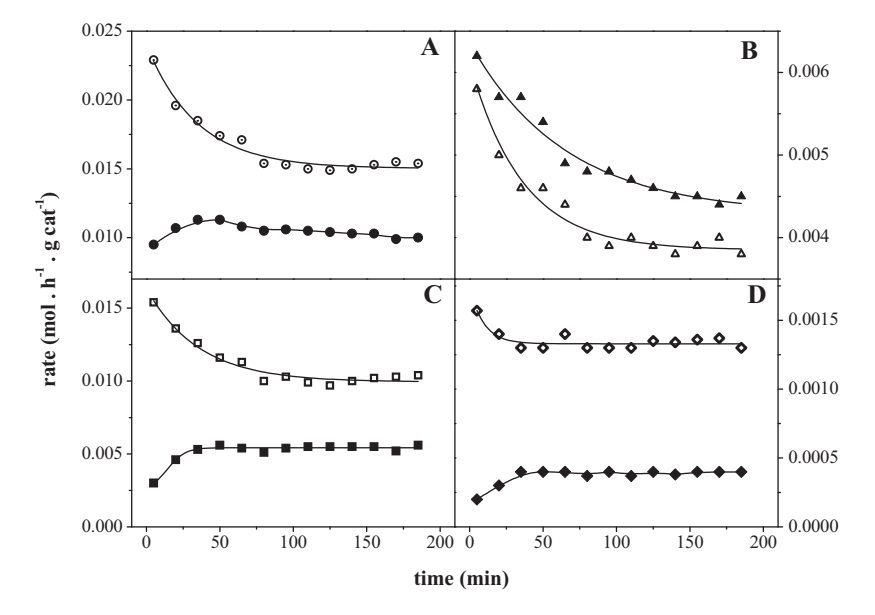


Fig. 4. Reaction rates of succinic anhydride conversion (A) and GBL (B), propionic acid (C) and methane (D) productions at $170 \,^{\circ}$ C over Ni/SiO₂ (full symbols) and Co/SiO₂ (open symbols). P = 1 bar, $W/F_{MA}^0 = 11.9$ g catalyst h mol⁻¹, $H_2/MA = 130$.

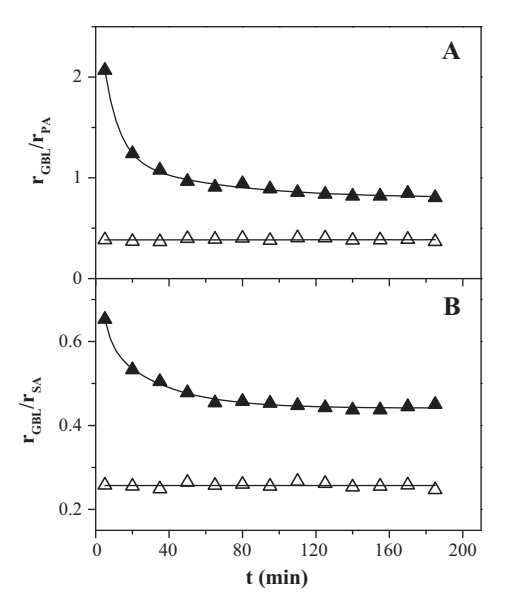


Fig. 5. Ratio between GBL and PA formation rates (A) and between GBL formation and SA conversion rates (B) at $170 \,^{\circ}\text{C}\,\text{over}(\blacktriangle)\,\text{Ni/SiO}_2, (\Delta)\,\text{Co/SiO}_2$. P = 1 bar, W/F_{MA}^0 = 11.9 g catalyst h mol $^{-1}$, H $_2/\text{MA}$ = 130.

experiment, the active sites for SA hydrogenolysis into PA were practically not deactivated. The last type of site could be the same for GBL hydrogenolysis into PA and CH₄. When Co/SiO₂ was used as catalyst, the hydrogenolysis rates diminished with time on stream in similar way (Fig. 4B-D). Now, $r_{GRI}/r_{PA} \cong 0.5$ and it kept practically constant during the 3 h reaction test, which is indicating that GBL production and PA production rates diminished in a similar way with time on stream (Fig. 5A). In other words, no selective deactivation was observed when Co/SiO₂ was used as catalyst at 170 °C. Besides, only 30% of the SA was converted to GBL with Co/SiO₂ (Fig. 5B). In summary, the results obtained at 170 °C and atmospheric pressure showed that the catalytic performance of Ni/SiO₂ and Co/SiO₂ for the MA hydrogenation and SA hydrogenolysis in gas phase was different. On one hand, Ni/SiO₂ was less active for SA hydrogenolysis but more selective to GBL and more stable than Co/SiO₂. On the other hand, the hydrogenolytic sites on metallic nickel and cobalt surfaces are deactivated in different way. A probable explanation is that more than one type of hydrogenolytic sites is present on the metallic surface of these catalysts.

The trends obtained at 220 °C were completely different to that observed at 170 °C. At 220 °C, Ni/SiO₂ was now some more active in the SA hydrogenolysis than Co/SiO2 (Fig. 3). Besides, the evolutions of SA conversion rates with time depend on the metal and temperature (Figs. 4A and 6A). At 220 °C, with both catalysts, SA conversion rate clearly increased with time on stream until a steady state was reached after about one hour (Fig. 6A). However, in the case of Co/SiO₂, a slow decrease in the SA conversion rate was observed after 2h on stream. In general, for both catalysts, PA and CH₄ production rates followed a similar evolution to that of SA conversion rate (Fig. 6A, C and D). The increase in PA and CH₄ production rates with time on stream was more pronounced with Co/SiO₂ than in the case of Ni/SiO₂ (Fig. 6C and D). The initial increase in the PA and CH₄ rates may be explained considering that SA adsorption on this type of hydrogenolytic sites is the controlling step. Thus, as the SA surface concentration increased, the PA and CH₄ production rates also increased, until the SA surface concentration reached a steady state after one hour on stream. Instead, GBL production rate showed a behavior completely different to those previously described for PA and CH₄. The GBL production rate kept constant with Ni/SiO₂ while it diminished almost linearly for Co/SiO₂ (Fig. 6B). Metallic cobalt sites involved in SA hydrogenolysis into GBL are initially more active than metallic nickel sites. However, metallic cobalt sites are deactivated during the catalytic test at 220 °C while metallic nickel sites do not suffer any important loss of activity. Thus, the initial r_{GBL}/r_{PA} and r_{GBL}/r_{SA} ratios were initially higher with Co/SiO₂ than with Ni/SiO₂ but they reached similar steady state at the end of the run (Fig. 7A and B). These results are in agreement with those obtained with Ni/SiO2 at 170 °C, showing that hydrogenolysis reactions to give GBL and PA are following parallel pathways and they occur on different type of metallic sites.

In summary, Ni/SiO_2 and Co/SiO_2 catalysts are active to produce GBL and PA by SA hydrogenolysis. Even more, both catalysts are more active for gas-phase hydrogenolysis and decarbonylation of SA than metal copper [20]. However, Ni/SiO_2 was more stable than Co/SiO_2 for the selective hydrogenolysis of SA into GBL.

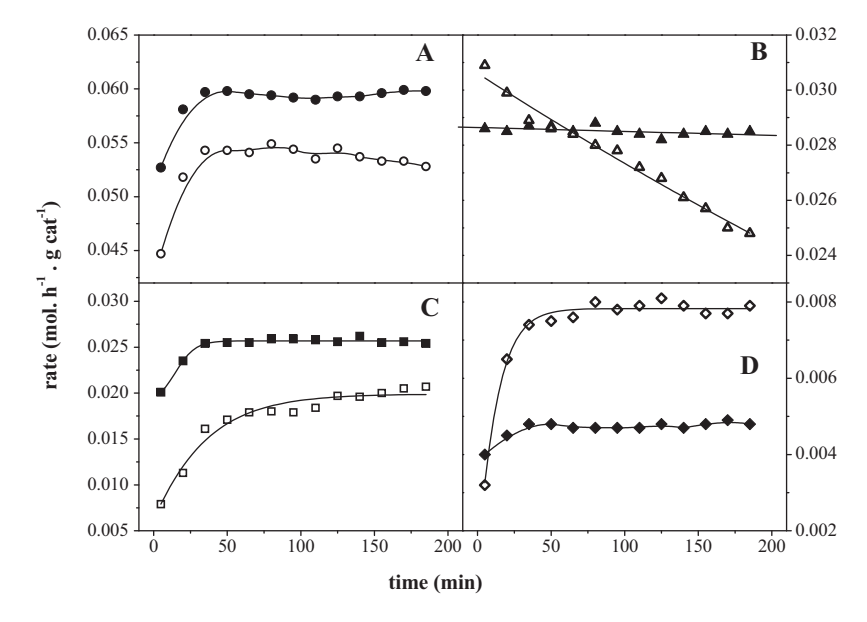


Fig. 6. Reaction rates of succinic anhydride conversion (a) and GBL (b), propionic acid (c) and methane (d) productions at $220\,^{\circ}\text{C}$ over Ni/SiO₂ (full symbols) and Co/SiO₂ (open symbols). P=1 bar, $W/F_{MA}^0=11.9\,\text{g}$ catalyst h mol $^{-1}$, H₂/MA=130.

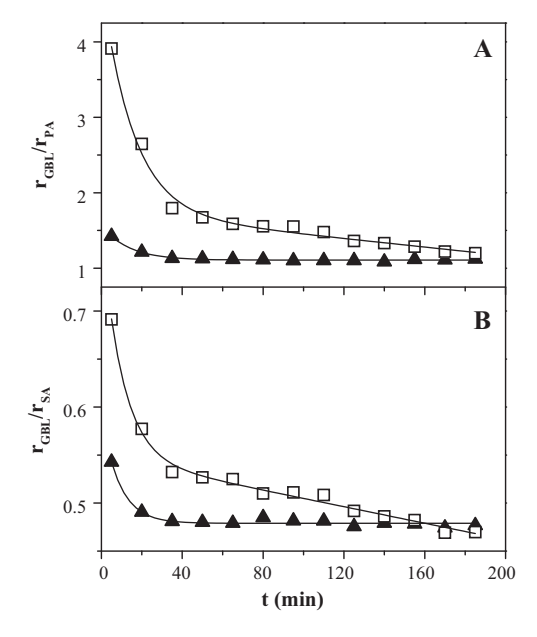


Fig. 7. Ratio between GBL and PA formation rates (A) and between GBL formation and SA conversion rates (B) at 220 °C. P = 1 bar, $W/F_{\rm MA}^0 = 11.9$ g catalyst h mol⁻¹, $H_2/MA = 130$. (\blacktriangle) Ni/SiO₂, (\square) Co/SiO₂.

3.3. Temperature-programmed oxidation

In a previous work, the deactivation of Ni(Pt)/HY-Al₂O₃ in the gas-phase MA hydrogenation at 40 °C and 8 bar was attributed to competitive adsorption of H₂O [21]. However, the only evidence to support the former assumption was an experiment carried out at 110 °C and 10 bar. In this experiment, the MA conversion was 100% during the whole experiment. On this basis, the authors affirmed that no deactivation was observed because H2O was removed at 110 °C and 10 bar. However, no evidence to rule out coke deposition during the hydrogenation reaction was reported in that work. Besides, the fact that MA conversion remains constant at 100% is not enough to discard deactivation of the catalytic bed. In order to get more information on the possible causes of catalyst deactivation during the gas-phase hydrogenation of MA over Ni/SiO₂ and Co/SiO₂ catalysts, temperature-programmed oxidation (TPO) experiments were carried out. After reaction at 170 and 220 °C, the catalyst samples were analyzed by TPO. The results are summarized in Table 3 and Fig. 8.

The total coke deposited on the catalyst surface was always higher on Co/SiO_2 than on Ni/SiO_2 (Table 3). In the case of Ni/SiO_2 , the total coke was similar at 170 and 220 °C. Instead, with Co/SiO_2 , the total coke was 10% lower at 220 °C than at 170 °C. It is probably that the diminution in total coke is due to hydrogenation and hydrogenolysis of coke precursors, which clean the catalyst surface. Since the reaction rate increases with temperature, then these hydrogenation and hydrogenolysis reactions becomes more noticeable at 220 °C than at 170 °C. The same phenomenon was observed in the gas-phase MA hydrogenation with Cu/SiO_2 [20].

Table 3Coke content determined by temperature-programmed oxidation (TPO) after gasphase hydrogenation of maleic anhydride (*P* = 1 bar).

Catalyst	T(°C)	Total coke (%)	Coke (LT) ^a (%)	
Ni/SiO ₂	170	1.6	1.6	
	220	1.6	1.3	
Co/SiO ₂	170	3.4	2.9	
	220	3.0	2.0	

^a Coke burnt at T < 350 °C.

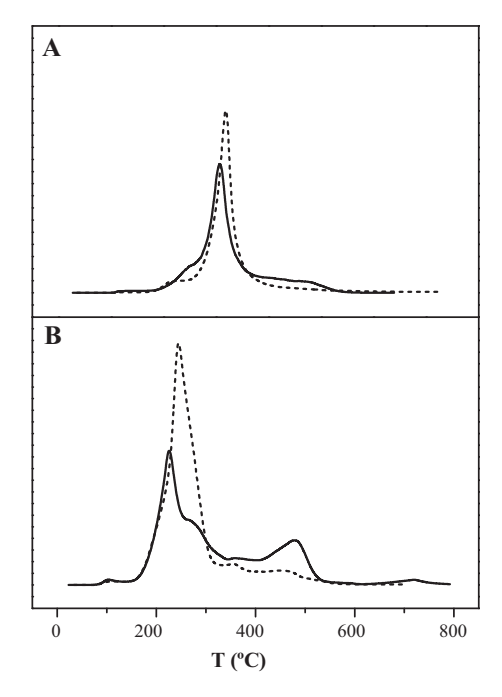


Fig. 8. TPO profiles of used catalysts. Ni/SiO $_2$ (A), Co/SiO $_2$ (B). Dash lines: TPO after reaction at 170 °C. Full lines: TPO after reaction at 220 °C.

Two well differentiated zones are observed in the TPO profiles (Fig. 8): (a) O_2 uptake peaks at T < 350 °C; (b) a broader and less intense O_2 consumption peak at T > 350 °C. According to literature data [28,29], these O_2 consumption peaks may be assigned to: (a) reactive and/or product molecules very strongly adsorbed on the metal surface (CP₁)[20]; (b) coke precursor and/or amorphous coke formed from the reactive and/or products strongly adsorbed on the metal surface (CP2). In both cases, the burning of these carbonaceous deposits can be catalyzed by the metal particles. For both Ni/SiO₂ and Co/SiO₂, the O₂ consumption at T>350 °C increased with reaction temperature at expense of the lower temperature peaks (Table 3 and Fig. 8A and B). Then, CP₁ react on the metal surface to form more stable coke species (CP2). The relative increase of the peak at T > 350 °C was more important in the case of the Co/SiO₂ (Fig. 8B) than for the Ni/SiO₂ catalyst (Fig. 8A). In other words, conversion of CP₁ into CP₂ is easier on Co/SiO₂ than on Ni/SiO₂.

On the basis of the former results, it is proposed that: (1) the catalyst deactivation is due to carbonaceous species deposited on the metal surface; (2) the higher stability of Ni/SiO_2 respect to Co/SiO_2 may be attributed to the lower amount of the total carbonaceous species deposited on the catalyst surface.

The results obtained at $170\,^{\circ}\text{C}$ on Ni/SiO₂ (Fig. 4) and at $220\,^{\circ}\text{C}$ on Ni/SiO₂ and Co/SiO₂ (Fig. 6) showed that GBL and PA production rates followed different evolutions with time on stream. This is in agreement with the fact that coke precursors are deactivating more the metallic sites active for SA hydrogenolysis into GBL than those active for the hydrogenolysis of SA into PA.

All these results are in agreement with the pattern observed for the SA hydrogenolysis reaction: $Co/SiO_2 > Ni/SiO_2 > Cu/SiO_2$.

4. Conclusions

Ni/SiO $_2$ and Co/SiO $_2$ catalysts, having low metal dispersion and low metal-support interaction, were active in both the selective hydrogenation of maleic anhydride and the hydrogenolysis of succinic anhydride in gas phase, at atmospheric pressure and 170–220 °C. In all of the cases, the main products of succinic anhydride hydrogenolysis were γ -butyrolactone and propionic acid. The

relative amounts of these two products and the yield evolutions with time on stream were dependent on the nature of the metal phase and the experimental conditions.

Succinic anhydride was converted into γ -butyrolactone and propionic acid following parallel pathways. In general, the evolutions with time on stream, for the production rates of γ butyrolactone and propionic acid, were different. This last is in agreement with the fact that the two hydrogenolysis reactions took place on two different types of metallic sites. The active sites involved in the hydrogenolysis of succinic anhydride into γ butyrolactone were deactivated more easily than those involved in the hydrogenolysis of succinic anhydride into propionic acid. The deactivation of the hydrogenolytic sites was due to deposition of carbonaceous compounds over the metal surface. The amount of carbonaceous residues was lower on Ni/SiO2 than on Co/SiO₂, which is in agreement with the highest catalytic stability of the Ni-based catalyst in the hydrogenolysis of succinic anhydride into γ-butyrolactone. The ratio between the rate for carbon compounds deposition and the rate of surface cleaning reactions, to keep approximately constant the hydrogenolytic activity along the time, seems to be the ideal in the case of Ni/SiO₂.

Acknowledgments

We thank the Universidad Nacional del Litoral (UNL), Consejo Nacional de Investigaciones Científicas y Técnicas (CONICET) and Agencia Nacional de Promoción Científica y Tecnológica (ANPCyT), Argentina for the financial support of this work.

References

[1] Y.Zhu, J. Yang, G. Dong, H. Zheng, H. Zhang, H. Xiang, Y. Li, Appl. Catal. B: Environ. 57 (2005) 183–190.

- [2] G. Budroni, A. Corma, J. Catal. 257 (2008) 403-408.
- [3] P. Boyaval, C. Corre, Lait 75 (1995) 453-461.
- [4] R.P. Patil, A.A. Kelkar, R.V. Chaudhari, J. Mol. Catal. 72 (1992) 153–165.
- W. Lu, G. Lu, Y. Guo, Y. Guo, Y. Wang, Catal. Commun. 4 (2003) 177–181.
 D. Zhang, H. Yin, R. Zhang, J. Xue, T. Jiang, Catal. Lett. 122 (2008) 176–182.
- [7] Y. Zhu, G. Zhao, J. Chang, J. Yang, H. Zheng, H. Xiang, Y. Li, Catal. Lett. 96 (2004)
- 123–127.
- [8] J.H. Schlander, T. Turek, Ind. Eng. Chem. Res. 38 (1999) 1264-1270.
- [9] Y.-L. Zhu, H.W. Xiang, G.S. Wu, L. Bai, Y.W. Li, Chem. Commun. (2002) 254–255.
- [10] S.M. Jung, E. Godard, S.Y. Jung, K.C. Park, J.U. Choi, Catal. Today 87 (2003) 171–177.
- [11] T. Hu, H. Yin, R. Zhang, H. Wu, T. Jiang, Y. Wada, Catal. Commun. 8 (2007) 193–199.
- [12] A. Messori, A. Vaccari, J. Catal. 150 (1994) 177-185.
- [13] G. Castiglione, M. Ferrari, A. Guercio, A. Vaccari, R. Lancia, C. Fumagalli, Catal. Today 27 (1996) 181–186.
- [14] U.R. Pillai, E. Sahle-Demessie, D. Young, Appl. Catal. B: Environ. 43 (2003) 131–138.
- [15] S.H. Vaidya, C.V. Rode, R.V. Chaudari, Catal. Commun. 8 (2007) 340-344.
- [16] S.M. Jung, E. Godard, S.Y. Jung, K.C. Park, J.U. Choi, J. Mol. Catal. A: Chem. 198 (2003) 297–302.
- [17] C. Gao, Y. Zhao, D. Liu, Catal. Lett. 118 (2007) 50-54.
- [18] L. Pu, L. Ye, Y. Yuanqi, J. Mol. Catal. A: Chem. 138 (1999) 129-133.
- [19] H. Jeong, T.H. Kim, K.I. Kim, S.H. Cho, Fuel Proc. Technol. 87 (2006)
- [20] C.I. Meyer, A.J. Marchi, A. Monzon, T.F. Garetto, Appl. Catal. A: Gen. 367 (2009) 122–129.
- [21] J. Li, W.-P. Tian, L. Shi, Catal. Lett. 141 (2011) 565-571.
- [22] J. Li, W.-P. Tian, L. Shi, Ind. Eng. Chem. Res. 49 (2010) 11837-11840.
- [23] T.F. Garetto, E. Rincón, C.R. Apesteguía, Appl. Catal. B: Environ. 48 (2004) 167–174.
- [24] R. Frety, L. Tournayan, M. Primet, G. Bergeret, M. Guenin, J. Baumgartner, A. Borgna, J. Chem. Soc. Faraday Trans. 89 (1993) 3313–3318.
- [25] H.F.J. Van't Blik, R. Prins, J. Catal. 97 (1986) 188-199.
- [26] C.I. Meyer, PhD Dissertation, Universidad Nacional del Litoral, 2009.
- [27] N.M. Bertero, A.F. Trasarti, C.R. Apesteguía, A.J. Marchi, Appl. Catal. A: Gen. 394 (2011) 228–238.
- [28] S.C. Fung, C.A. Querini, J. Catal. 138 (1992) 240-248.
- [29] E.L. Rodrigues, A.J. Marchi, C.R. Apesteguía, J.M.C. Bueno, Appl. Catal. A: Gen. 294 (2005) 197–207.